GeoScienceWorld
Lithosphere
Volume 2022, Article ID 7349759, 15 pages
https://doi.org/10.2113/2022/7349759

Lithosphere

Research Article

Precursor Information Recognition of Rockburst in the Coal-Rock Mass of Meizoseismal Area Based on Multiplex Microseismic Information Fusion and Its Application: A Case Study of Wudong Coal Mine

Huicong Xu,[1] **Xingping Lai**,[1,2] **Shuai Zhang**,[1] **Pengfei Shan**,[1,2] **Zheng Wu**,[1] **Haidong Xu**,[1] **Rui Bai**,[1] **and Qifeng Guo**[1,3]

[1]*School of Energy Resources, Xi'an University of Science and Technology, Xi'an 710054, China*
[2]*State Key Laboratory of Green low Carbon Development of Oil-Rich Coal in Western China, Xi'an 710054, China*
[3]*School of Civil and Resource Engineering, University of Science and Technology Beijing, Beijing 100089, China*

Correspondence should be addressed to Huicong Xu; xhcxust@163.com and Shuai Zhang; zscsy1993@163.com

Received 7 May 2022; Accepted 7 July 2022; Published 20 July 2022

Academic Editor: Shaofeng Wang

In recent years, the rockburst induced by steeply inclined coal seam mining in the Urumqi mining area has become serious. In this paper, the evolution law of multiplex microseismic information before and after the rockburst is obtained through in-depth mining of the field microseismic data. In addition, the evolution characteristics of microseismic activities before and after the rockburst of steeply inclined coal-rock mass in the meizoseismal area are revealed from three important scales: time, space, and strength. The results show the following: (1) The microseismic activity of the Wudong Coal Mine is mainly of stress migration type. The sandwiched rock pillar is the primary inducement of rockburst, and the *b* value decreases greatly with the mining progresses (by 23.9%). It indicates that the risk of rockburst induced by the local failure of rock mass in this area is increasing. (2) From the time scale and strength index, the precursory indexes of rockburst are put forward, respectively: ① the daily total energy and the frequency of microseisms suddenly rise and fall rapidly at the same time in the shock start-up period (5 days before rockburst), and the daily total energy of microseisms decreases to the abnormal valley value within 30 days. ② The abnormal growth rate of microseismic events exceeded 60% in a certain stage, and "induced shock events" appeared. (3) The shock risk is positively correlated with the decline rate of energy index, the growth rate of cumulative apparent volume, and Schmidt. It is determined that the rockburst will occur within 19 days after entering the shock early warning period. The results of prediction examples show that this method has a good prediction effect on rockburst in strong meizoseismal areas, which can provide a reference for rockburst prevention in the mining process in strong meizoseismal areas.

1. Introduction

As one of the large coal bases constructed in China's "The New Silk Road" economic belt, Xinjiang has a large number of steeply inclined extrathick coal seams [1]. With the continuous increase of mining scale and depth, rockburst has become the primary problem restricting the safe development in the Urumqi mining area of Xinjiang [2]. Xinjiang is one of the provinces with the most frequent strong seismicities in China. Urumqi mining area is located in the Tianshan seismic belt, a total of 359 earthquakes with $M \geq 5$ occurred from 1900 to 2007. There were 1 M8 earthquake, 9 M7 earthquakes, 62 M6 earthquakes, and 287 M5 earthquake [3]. Wudong Coal Mine, located in this meizoseismal area, is a typical steeply inclined extrathick coal seam mine. In recent years, several serious rockbursts have occurred (Table 1). At present, the mechanism of rockburst has not been unified [4–6]. It is even more unrealistic to realize the early warning of rockburst in meizoseismal areas only through theoretical analysis or numerical simulation. Therefore, the

Table 1: Historical rockbursts in the south mining area of Wudong Coal Mine.

Number	Date	Released energy (J)	Event location
1	2013.07	2.0×10^7	+500 level B_{3+6} working face
2	2014.03	2.1×10^7	+506 level sandwiched rock pillar
3	2015.03	4.9×10^8	+487 level sandwiched rock pillar
4	2015.07	9.0×10^7	+470 level sandwiched rock pillar
5	2016.11	9.5×10^6	+460 level sandwiched rock pillar
6	2017.02	2.1×10^8	+460 level B_6 roof
7	2017.04	2.2×10^6	+431 level sandwiched rock pillar

in-depth mining of field-measured data should be strengthened to realize the effective early warning of the rockburst of the Wudong Coal mine in the meizoseismal area.

At present, many scholars have done a lot of research on the evolution laws of microseismic data of coal-rock mass instability failure. Zhang et al. [7], aiming at the problem of low efficiency in artificial identification of stope instability early warning period in Shaba Mine, realized the intelligent prediction of the critical state of rock mass instability by introducing the microseismic activity parameters of the stope. Dong et al. [8] established a velocity-free MS/AE source location method for three-dimensional structures with holes by introducing an A^* search algorithm based on equidistant grid point search paths. This can effectively predict and prevent the structure of potential hazard sources. Li et al. [9] comprehensively analyzed the critical conditions for bending and fracturing the regenerated roof during mining. Meanwhile, by applying continua FLAC-3D numerical simulation, this research simulated changes in the stress and strain on a regenerated roof during mining and proposed prevention and control methods for dynamic disasters. Zhang et al. [10] carried out a multidimensional display and in-depth statistical analysis of microseismic data of a mine in Shandong. The potential dangerous areas were located, and the shock risk level was evaluated from the time and space scales. Xue et al. [11] analyzed the evolution law of microseismic activity parameters such as cumulative apparent volume, energy index, and cumulative release energy before and after rockburst in the Shuangjiangkou hydropower station tunnel. They achieved an accurate prediction of the warning period and construction safety period through the proposed lgN/b index. Wang et al. [12] analyzed the frequency of microseismic events before and after each rockburst, daily microseismic energy, energy index, cumulative apparent volume, and E_s/E_p value. The microseismic precursor characteristics of two intermittent rockbursts are further revealed. Cheng et al. [13], based on the microseismic data measured in the field, focused on the "time-space" evolution law of the precursory index of the dynamic instability of coal-rock mass based on the multivariate indexes such as the location, frequency, and energy level of the microseismic events in the field. Lai et al. [14, 15], based on the 'energy-frequency' variation law of MS data of coal-rock mass failure and instability during mining, predicted the tendency area of pillar dynamic instability.

The above research mainly focuses on the analysis of microseismic parameters of coal-rock mass in underground engineering. However, there are few research results at home and abroad on the "time-space-intensity" evolution law of microseismic events and the precursory characteristics of shock instability based on field data. In particular, the precursor identification and early warning of shock instability of steeply inclined coal-rock mass in meizoseismal area based on multivariate microseismic information fusion. Therefore, by deeply mining the historical microseismic data of the Wudong Coal Mine, this paper mastered the response law of the precursor index of impact instability and the shock risk of key areas (sandwiched rock pillar) based on the fusion of multiplex microseismic information. The shock warning period and shock disaster-causing time of key areas were determined. This provides a scientific basis for safe and efficient mining of steeply inclined extrathick coal seams after entering deep mining.

2. Engineering Background

2.1. Mine Mining Conditions. The design production capacity of the Wudong Coal Mine is 6.0 Mt/a. The main coal seams of the Wudong Coal Mine are the B_{1+2} coal seam and B_{3+6} coal seam. They are steeply inclined extrathick coal seams with medium hardness and weak outburst proneness. The average thickness of the B_{1+2} coal seam is 35 m and that of the B_{3+6} coal seam is 45 m. Their average angles are 87°. There is a hard rock pillar between the two seams with a thickness of 50 m-110 m. The horizontal section fully mechanized top-coal caving mining method is used in Wudong Coal Mine. The length of the working face is the thickness of the coal seam. During mining operations, the B_{1+2} coal seam usually lags behind the B_{3+6} coal seam by one subsection height. The +425 level B_{3+6} working face is currently mined in the southern mining area of the Wudong Coal Mine. Above the +425 level B_{3+6} working face is the +450 level B_{3+6} working face, and below is the +400 level working face. The occurrence characteristics and mining layout of the steeply inclined coal-rock mass in the southern mining area are shown in Figure 1.

2.2. Geological Condition of Coal Mine. Affected by the collision between the Indian plate and Eurasian plate, the crust in the western region is strongly squeezed. This geodynamic mechanism of plate collision causes unique crustal

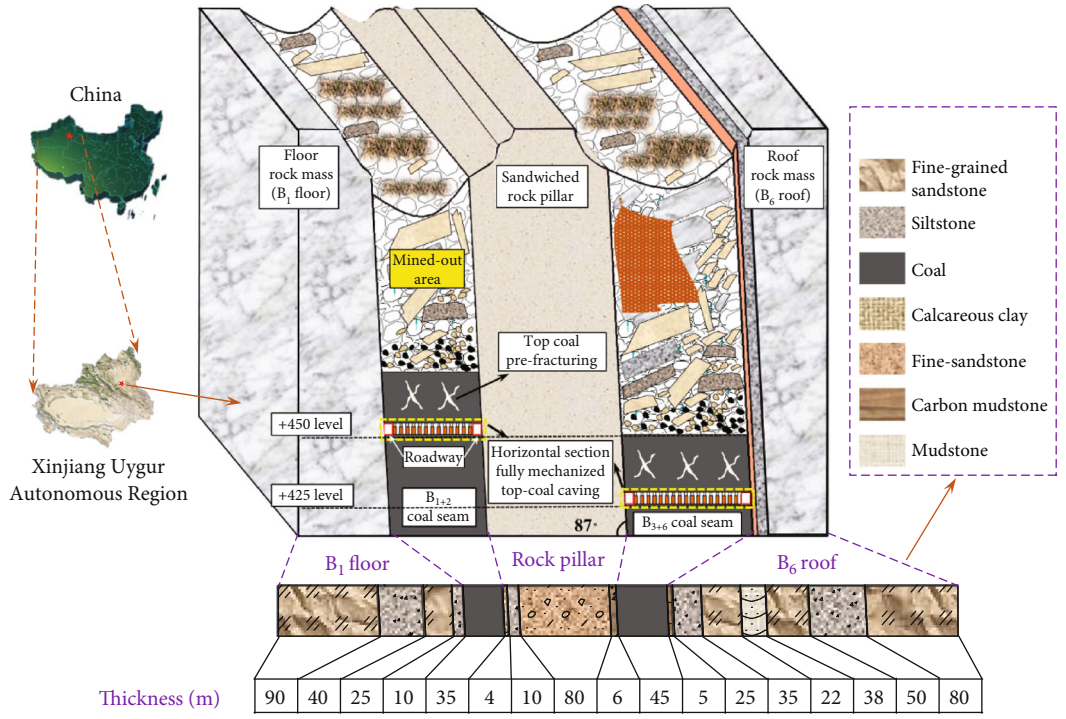

Figure 1: Stratum characteristics and mining layout of steeply inclined coal-rock mass.

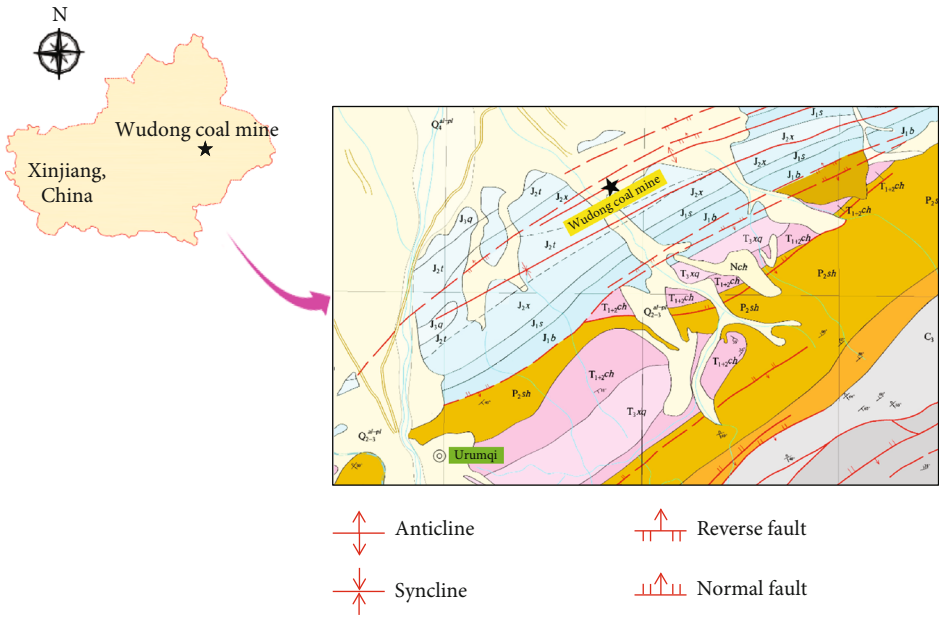

Figure 2: Geologic structure diagram of Wudong Coal Mine.

deformation and tectonic stress systems in western China. Wudong Coal Mine is located in the Urumqi mining area of Xinjiang. The Tianshan seismic belt is one of the 23 seismic belts in China, and it is also the most active tectonic belt in Xinjiang. Wudong Coal Mine is located in the central area of the northern Tianshan fold belt, which is a typical compressional tectonic activity area (Figure 2). At present, it is still under the influence of the Himalayan movement, and there is a strong residual tectonic stress. There are Badaowan syncline and Qidaowan anticline in the mining area. Badaowan syncline is relatively complete, and Qidaowan anticline is only the south wing. The lithology of the coal seam roof and the floor is mainly siltstone, fine sandstone, and mudstone, followed by carbonaceous mudstone. Most of the structural planes are bedding planes, which are prone to plastic deformation of bottom heave

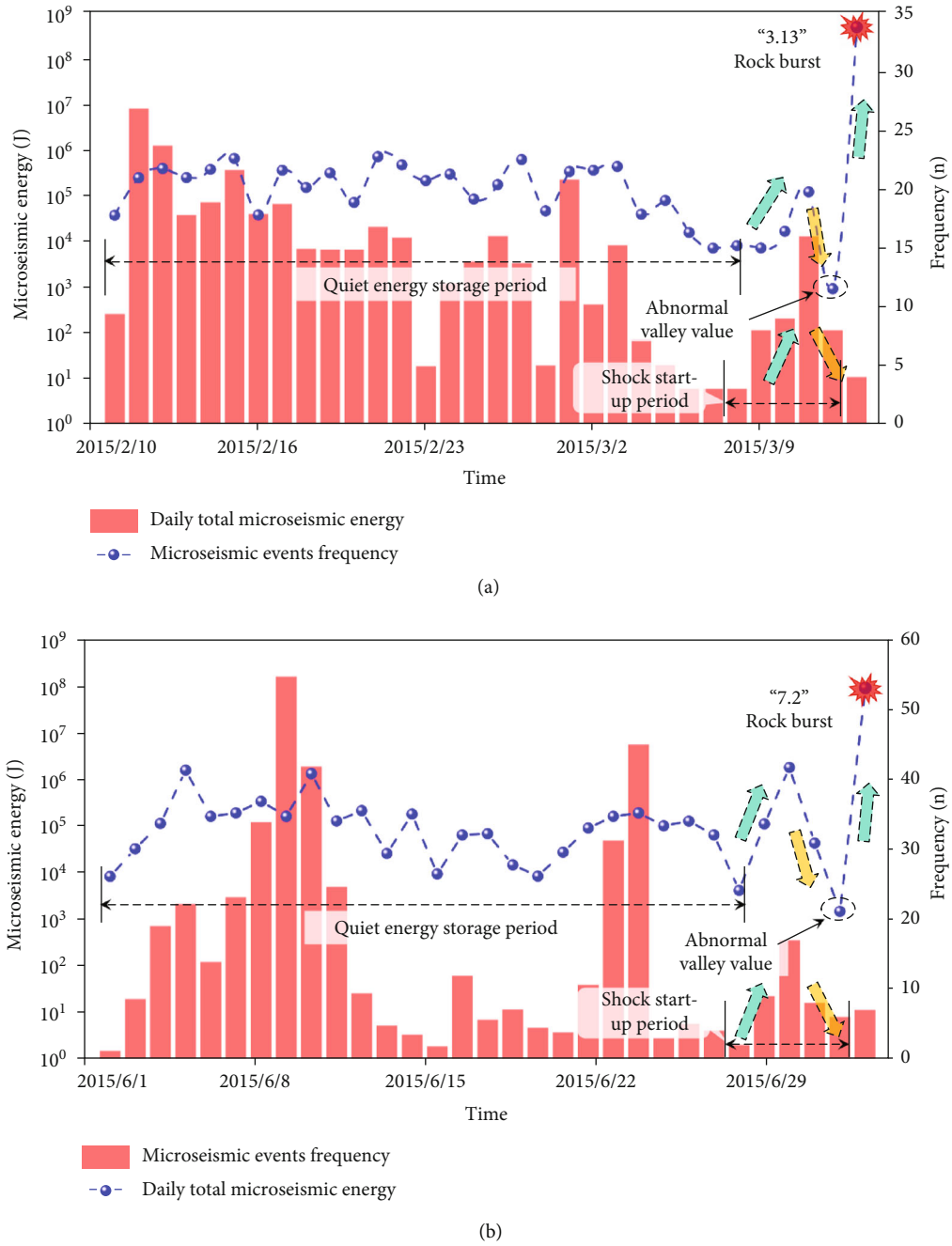

Figure 3: Characteristics of "energy-frequency" of microseismic events before two rockbursts. (a) "3.13" rockburst and (b) "7.2" rockburst.

and sidewall outburst, and may also cause a shear slip of block collapse and sliding. The maximum horizontal principal stress is consistent with the dip direction of the coal seam, and the minimum principal stress is along the direction of the coal seam. The field horizontal stress is 1.74-1.90 times vertical stress, which is a typical tectonic stress field [16].

3. "Time-Space-Strength" Evolution Law of Historical Rockbursts

Wudong Coal Mine adopts ARAMIS M/E microseismic monitoring equipment produced in Poland to integrate a digital DTSS transmission system. This system is composed of a ground part (ARAMIS M/E data processing computer, record server, and DTSS ground center station) and a field part (seismograph, NSGA transmitter, and microseismic probe). In recent years, seven rockburst accidents have occurred in the southern mining area, and the affected areas are all B_{3+6} working face areas. There were two rockbursts ("3.13", "7.2") when the energy was close to or more than 1×10^8 J. The disaster-causing factors of rockburst are complex. Deep mining the dynamic evolution law of microseismic data before rockburst is very important for disaster prevention and control. Therefore, based on the microseismic data before

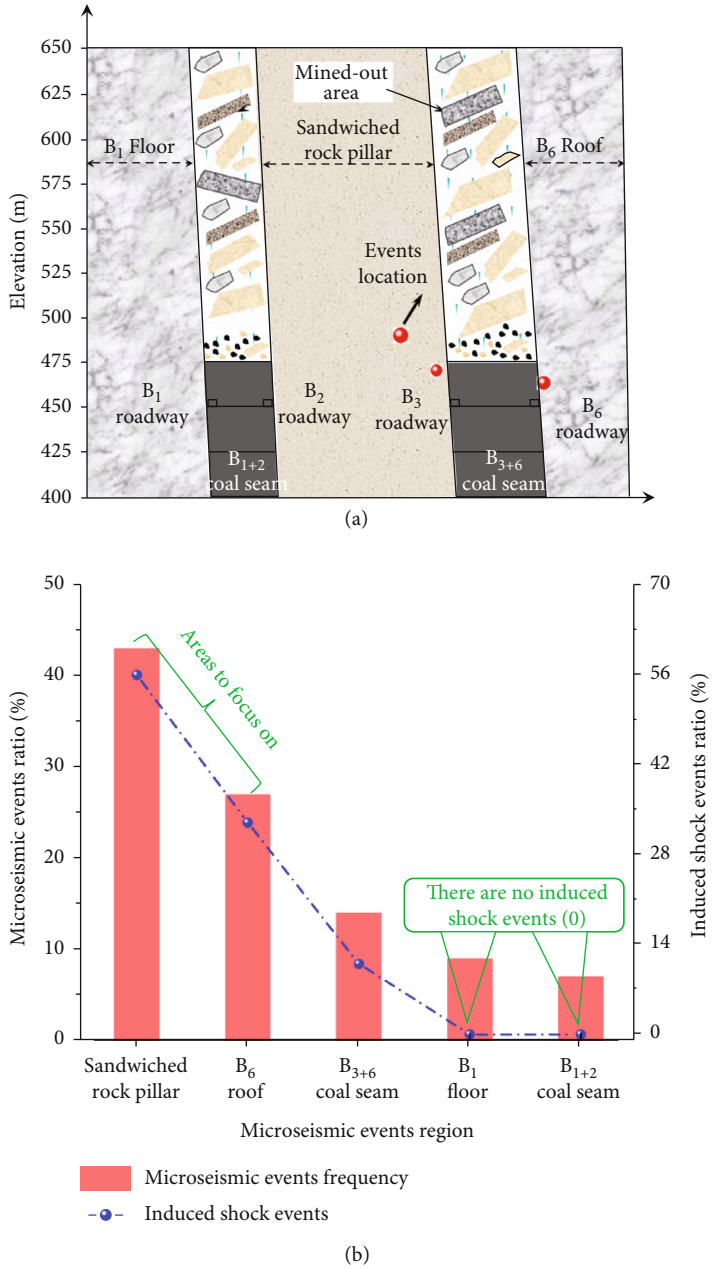

Figure 4: Distribution of (a) historical shock events and (b) ratio of microseismic events.

the two typical rockbursts, this section analyzes the characteristics of "time-space-strength" before and after the rockbursts in the southern mining area of the Wudong Coal Mine and realizes the multidimensional reflection of the precursor index of rockburst.

3.1. Time Characteristics of Historical Rockburst. In this section, the microseismic data of 30 days before the two rockbursts in the southern mining area are analyzed (Figure 3). We found that the energy and frequency of microseismic events showed an abnormal trend of the rapid rise and then rapid decline within 5 days before the rockburst. The two rockbursts occurred after the daily total energy of microseismic decreased to "abnormal valley value" (the minimum value of the energy before the rockburst). For example, (1) The microseismic energy and frequency in the southern mining area increased sharply during the mining process from 9 March to 11 March 2015. On March 12, the total energy and frequency of microseismic show a sharp downward trend. The daily total energy decreased to 1.3×10^3 J, and the minimum is 30 days. Subsequently, the energy value of 4.9×10^8 J rockburst occurred on March 13. (2) From June 27 to June 29, 2015, the total energy of microseismic events increased sharply, while from June 30 to July 1, 2015, the total energy of microseismic events decreased sharply. The daily total energy of July 1 is a minimum of 1.1×10^2 J in 30 days. The variation trend of microseismic frequency is consistent with that of microseismic energy.

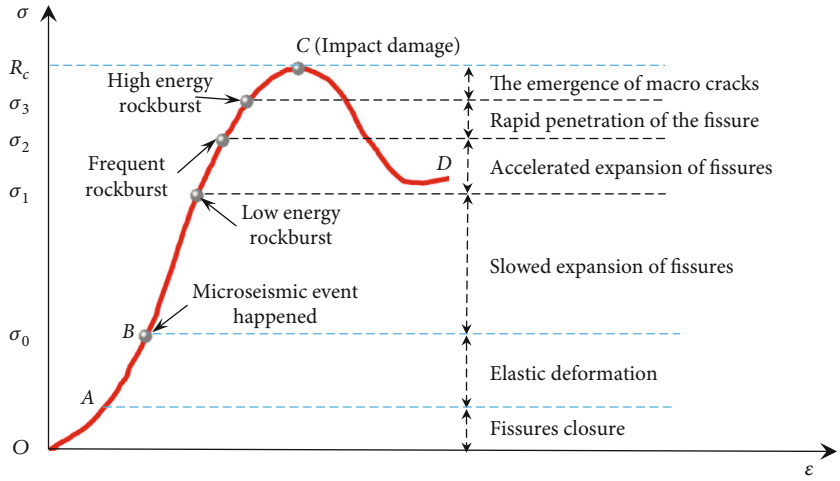

FIGURE 5: The response relationship between the stress-strain curve of typical rock failure process and impact instability in the Wudong Coal Mine.

During the period from 29 June to 2 July, the phenomenon of "rapid increase-rapid decrease" appeared, and then, the "7.2" rockburst with an energy value of 9×10^7 J occurred.

The variation trend of total daily energy of microseisms in the 5 days (defined as the shock initiation period) before the two rockbursts is the same as the total frequency, and both are at the valley value in the previous 30 days. The main reason is that with the continuous advancement of the working face, the surrounding rock produces a large number of microcracks, producing a large number of low-energy microseismic events. The energy and frequency in this stage are in a small fluctuation stage. However, the energy stored in the coal-rock mass is not enough to destroy the energy field balance at this stage. Coal-rock mass enters a period of "quiet energy storage period." During this period, the coal-rock mass is in a state of continuous energy accumulation. After entering the shock initiation period (the first 5 days of the rockburst), the energy accumulated in the coal-rock mass will reach the storage limit. At this time, the accelerated expansion of mining fractures release some energy, and the frequency of microseismic events increases. After that, the coal-rock mass entered a strong energy storage state again. The coal-rock mass in the state of strong energy storage is superimposed with the dynamic load caused by mining on the day of rockburst, which causes the sudden release of energy stored in the coal-rock mass and induces rockburst. According to the above analysis, the daily total energy and frequency of microseismic events suddenly show a rapid increase and a rapid decrease trend within 5 days, and the abnormal valley value of the total daily energy falling to 30 days can be used as one of the precursor indexes of rockburst.

3.2. Spatial Characteristics of Historical Rockburst. From the spatial position of seven rockbursts (Figure 4(a)), five of them occurred in the rock pillar near the B_{3+6} coal seam and one occurred in the B_6 roof. The shock failure phenomenon is dominated by the side drum of the roadway, indicating that the shock force source of the B_{3+6} coal seam is mainly concentrated on the two sides of the roadway (sandwiched rock pillar B_6 roof). From the deformation of surrounding rock, the south side of the roadway (sandwiched rock pillar) is significantly greater than the north side (B_6 roof side). From the point of the failure phenomenon, the front and rear columns of the working face near the B_3 roadway appear bending, and the shrinkage of "U"-shaped steel reaches 30 cm, which is far greater than that of the B_6 roadway.

By analyzing the microseismic events of 30 days before the seven rockbursts (Figure 4(b)), it is found that the area with the frequency of the highest event is the sandwiched rock pillar, accounting for 43% of the total event. Next are B_6 roof (27%), B_{3+6} coal seam (14%), B_1 floor (9%), and B_{1+2} coal seam (7%). In addition, a large number of field data show that most rockbursts occurred before the "inducing shock events" (energy greater than 10^6J) [17]. A total of 21 "inducing shock events" were monitored five days before the seven rockbursts. The proportion of "inducing shock events" in the rock pillar area was 55.6%, the proportion of B_6 roof is 33.3%, and the proportion of B_{3+6} coal seam is 11.1%. The above analysis shows that the rockburst in the south mining area has obvious spatial characteristics, and the rock pillar is the key disaster-causing area, which should be focused on.

3.3. Strength Characteristics of Historical Rockburst. With the gradual development of steeply inclined coal seam working face to the deep, the sandwiched rock pillar with both sides mined out and the isolated suspended B_6 roof shows a movement trend towards the goaf. The resulting "squeeze-prying" effect causes strong stress concentration in the coal-rock mass at the junction, which is also mutually verified with the location of the historical rockbursts.

We approximately consider the instability and failure phenomenon of steeply inclined coal-rock mass under the mining influence as the time-space evolution process of rheology to mutation. This process includes the development, expansion, and destruction of rock fracture, which also leads to the occurrence of microseismic events at various levels. The coal-rock mass with long-term high static load will produce different degrees of fractures affected by mining.

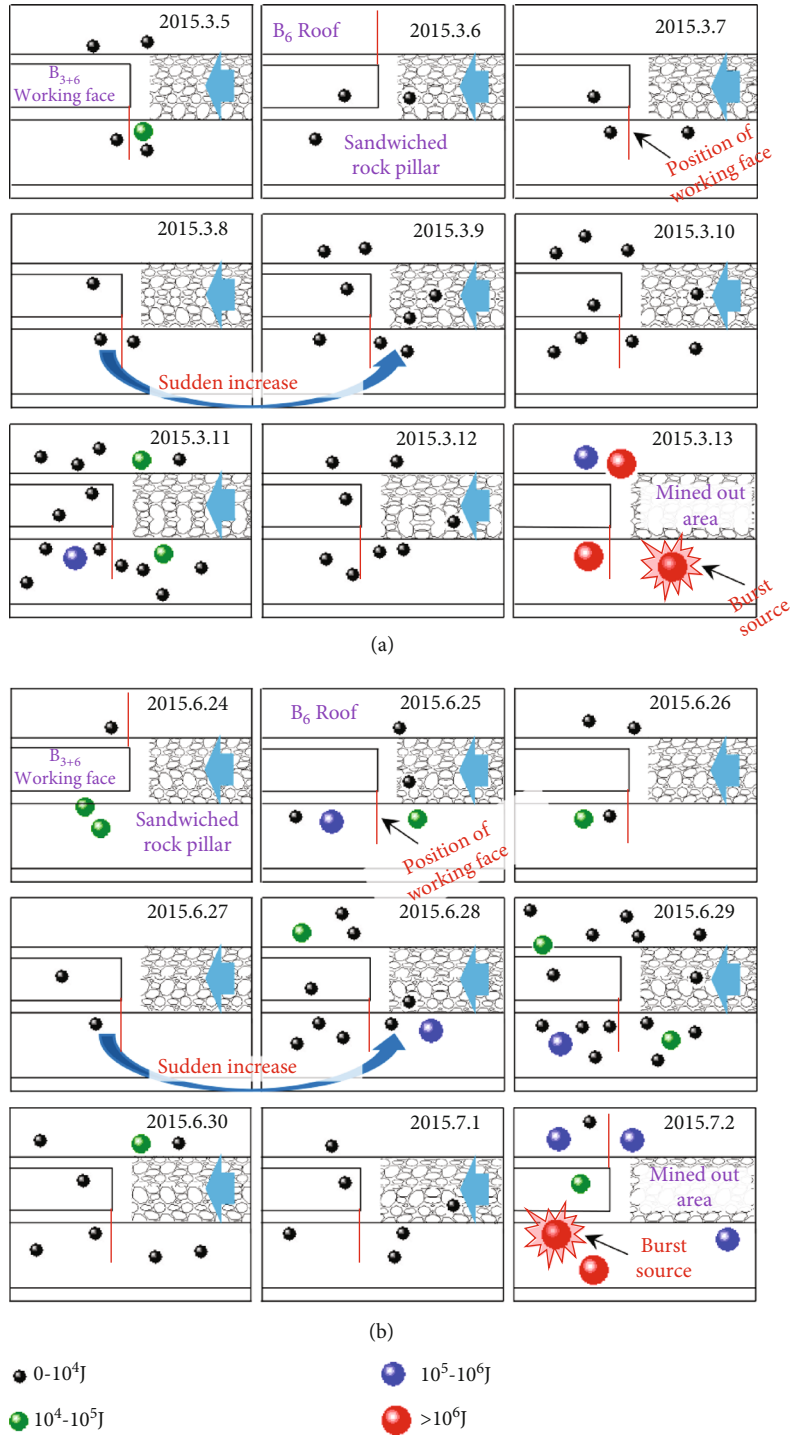

FIGURE 6: The "time-space-strength" evolution law of microseismic events in different energy ranges before rockburst. (a) "3.13" rockburst and (b) "7.2" rockburst.

During the occurrence of fracture development and expansion, the stored energy of coal-rock mass is released in the form of a vibration wave, thus generating a dynamic load.

The steeply inclined coal-rock mass will undergo four stages of deformation and failure during mining: fracture closure (OA), elastic deformation (AB), fracture propagation (BC), and shock failure (CD), as shown in Figure 5. Among them, the OB stage is mainly characterized by fracture closure and elastic deformation of coal-rock mass. At this stage, there is no damage and failure of coal-rock mass, and no new fractures are generated. The BC stage is mainly characterized by the gradual development, accelerated expansion, and rapid penetration of coal-rock fractures. Therefore, microseismic events mainly occur in the BD section. When the corresponding stress levels are in the ranges of (σ_0, σ_{b1}), $(\sigma_{b1}, \sigma_{b2})$, $(\sigma_{b2}, \sigma_{b3})$, and (σ_{b3}, R_C), different energy levels and frequencies

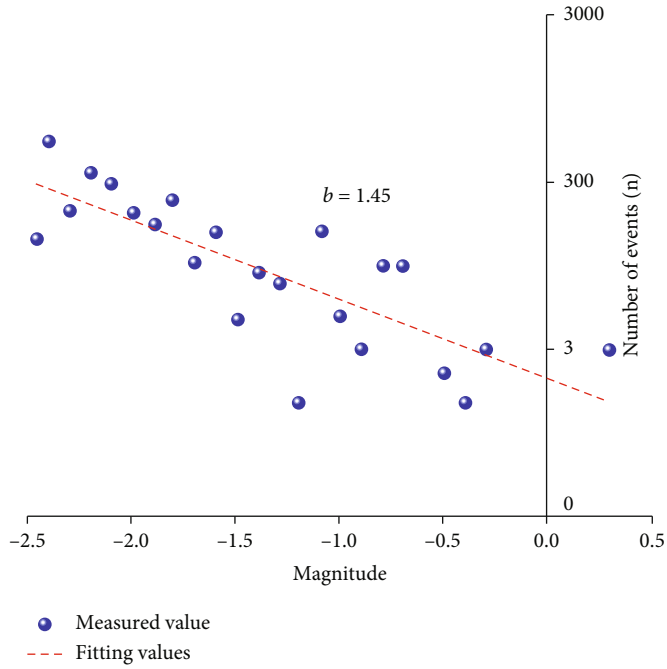

Figure 7: "Magnitude-frequency" relationship of microseismic events in the south mining area.

of mine earthquakes will occur. When the stress level exceeds the compressive strength of rock mass, large-scale microcracks are generated by fracture coalescence, and then, instability failure occurs [18, 19].

Frequent microseismic events indicate that the stress concentration in this area is high, and the shock risk is also higher than in other areas [20]. Based on the microseismic data 15 days before two rockbursts, this paper studies the evolution law of spatial distribution of seismic sources in stress concentration areas undermining influence. As shown in Figure 6, microseismic sources increased significantly and accumulated abnormally 3-4 days before the occurrence of rockburst. For the '3.13' rockburst, the daily average number of microseismic events before the abnormal increase of microseismic events was 3.5, while the daily average number of microseismic events during the abnormal accumulation period was 9, with a growth rate of 61.1%. For the '7.2' rockburst, the average number of microseismic events per day before the abnormal increase of microseismic events is 3.5, while the average number of microseismic events per day during the abnormal accumulation is 9.4, and the growth rate is 62.7%. The abnormal growth rates before the two rockbursts are all above 60%. This shows that the coal-rock mass in this region is in a very unstable state during the abnormal accumulation period before the rockburst, and a large number of cracks appear in the surrounding rock under the action of high concentrated stress. Microseismic events suddenly decreased within a few days before the occurrence of rockburst, the coal-rock in the 'strong storage period.' However, on the day of the rockburst, the source accumulated again in the stress concentration area. Microseismic events with an energy value of 1×10^3 J-1×10^4 J increased significantly, and 'induced shock events' (energy greater than 10^6J) occurred before the rockburst. These phenomena show that the energy stored in coal and rock mass in this area has been enough to destroy the existing balance, and the microcracks of coal-rock mass gradually penetrate and rupture. The accumulated energy of coal and rock mass is released instantly, inducing rockburst. Therefore, the abnormal growth rate of microseismic events in a certain stage is usually more than 60% and the 'induced shock event' can be seen as the spatial precursor index of rockburst in Wudong Coal Mine.

4. Analysis of Microseismic Activity Parameters in Different Space Regions

The large-scale regional monitoring function of the microseismic monitoring system has a good effect on the instability and early warning of surrounding rock [21]. The "time-space-strength" evolution laws of microseismic data before the two rockburst are analyzed, and it is found that there is a large risk of shock instability in the "sandwiched rock pillar-B_6 roof." Therefore, by analyzing the activity parameters such as the *b* value, energy index, cumulative apparent volume, and Schmidt of microseismic events before and after rockbursts, this section reveals the characteristics of microseismic activity parameters in different areas of the Wudong Coal Mine. Determine the shock time of "sandwiched rock pillar-B_6 roof" suitable for the south mining area, to provide theoretical support for the precursor early warning of coal-rock mass instability in the subsequent mining process.

4.1. Shock Risk Analysis of Different Space Areas. Relevant results show that microseismic events caused by mine excavation also follow Gutenberg Richter's law [22]. Therefore,

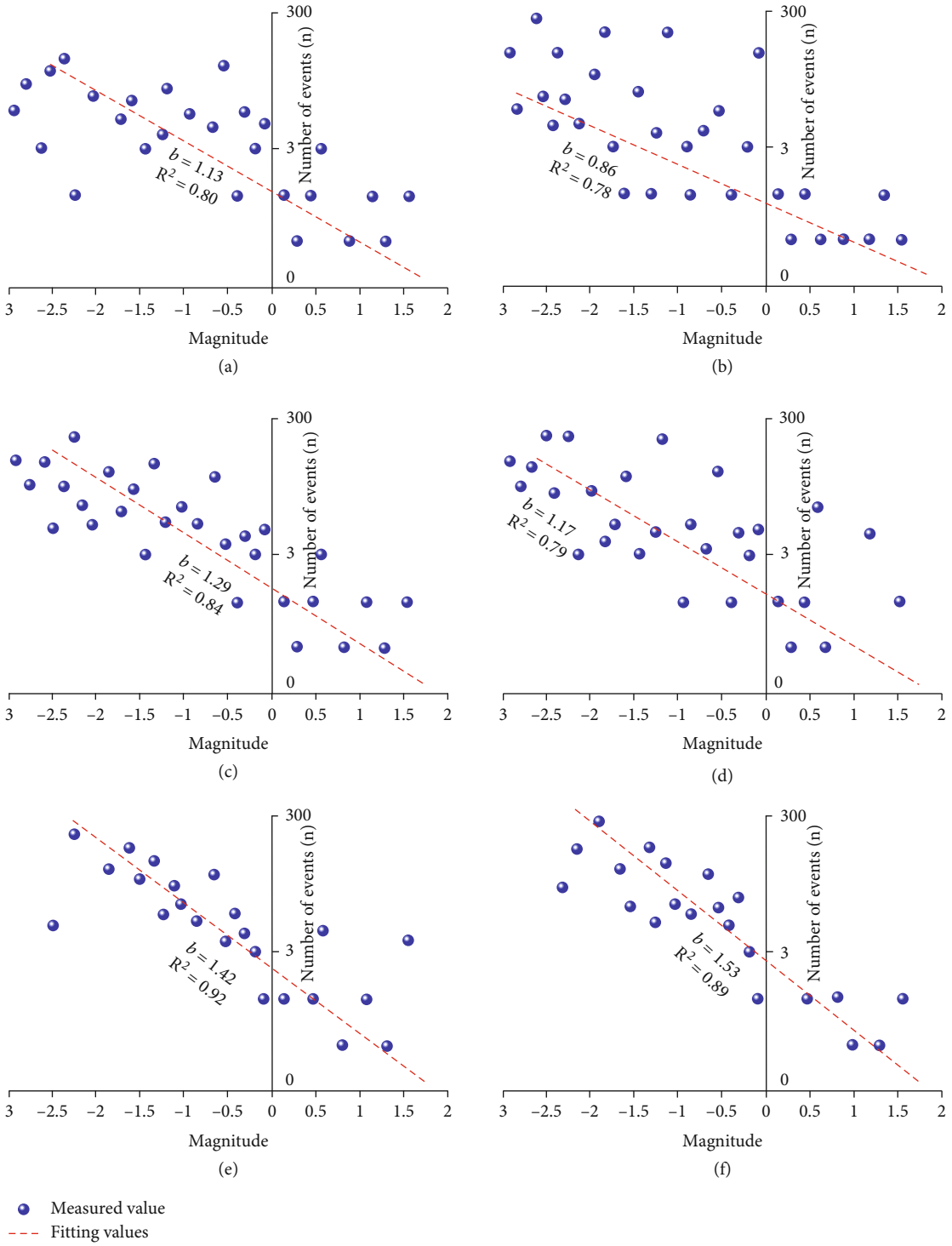

FIGURE 8: Variation of the b value of coal-rock mass in different areas under the mining influence. (a) b value of rock pillar in the first half-year, (b) b value of rock pillar in the whole year, (c) b value of B_6 roof in the first half-year, (d) b value of B_6 roof in the whole year, (e) b value of B_{3+6} coal seam in the first half-year, and (f) b value of B_{3+6} coal seam in the whole year.

the b value describing the distribution relationship of "magnitude-frequency" is also one of the important evaluation indexes of rockburst early warning. As shown in

$$lgn = a - bM, \tag{1}$$

where M is moment magnitude, n refers to the number of microseismic events greater than or equal to moment magnitude M, a represents the measurement of microseismic activity level, and b represents the relative proportional relationship between high-magnitude events and low-magnitude events in a certain period. When the mining coal

and rock mass is in the stable stage, the b value is large and relatively stable. When the rock mass fractures rapidly expand and penetrate and instability failure is about to occur, the b value decreases sharply. At the same time, the range of b values in different mines is different, which is determined by the source mechanism of the mine. The b value of fault slip microseismic event is small (less than 0.8), while the b value of mining stress migration microseismic activity is usually between 1.2 and 1.5 [23, 24].

Wudong Coal Mine is located in Tianshan seismic belt. Based on the evolution laws of the b value of onsite microseismic data, this section makes a quantitative study on the response characteristics of microseismic activity in the southern mining area. The microseismic event data of the southern mining area from January 1, 2016, to December 31, 2016 (no rock burst accident occurred at this stage) were extracted, and the b value at this stage was 1.45 (Figure 7). Therefore, we believe that the microseismic activity in the southern mining area is mainly of stress migration type. Mining stress migration plays a leading role in microseismic events, and faults and other geological structures have little influence.

In addition, to explore the b value evolution law of coal-rock mass in different areas of the south mining area, all microseismic data from January 1, 2016, to December 31, 2016, are selected for comparative analysis. The b value curves of microseismic events in different regions are shown in Figure 8. It can be seen that from January 1 to June 30, 2016, there were 2621 microseismic events in the rock pillars (Figure 8(a)), and the corresponding b value was 1.13. As of December 31, 2016, there were 4768 microseismic events in this area (Figure 8(b)), and the b value was 0.86. From January 1 to June 30, 2016, 1524 microseismic events occurred in the B_6 roof (Figure 8(c)), and the corresponding b value is 1.29. As of December 31, 2016, there were 2717 microseismic events in this area (Figure 8(d)), and the b value was 1.17. From January 1 to June 30, 2016, 676 microseismic events occurred in the B_{3+6} coal seam (Figure 8(e)), and the corresponding b value is 1.42. As of December 31, 2016, there were 1117 microseismic events in this area (Figure 8(f)), and the b value was 1.53.

During the monitoring period, the b value of the rock pillar and B_6 roof decreased in varying degrees with the mining. The b value of the rock pillar decreased by 23.9%. The b value of the B_6 roof is reduced by 9.3%. The b value of the B_{3+6} coal seam increased by 5.9%. Therefore, combined with the above analysis, it can be seen that the risk of local damage of coal-rock mass induced by microseismic events in the area with rock pillar and B_6 roof increases with the continuous progress of the working face. The shock risk of the rock pillar area is high, followed by the B_6 roof area. The shock risk of the B_{3+6} coal seam area is low. Therefore, real-time data analysis and evaluation should be carried out on the rock pillar in the field of rockburst prevention and control, and corresponding pressure relief measures should be carried out in time.

4.2. b Value Characteristics of Key Areas for Rockburst Prevention and Control. Through the data analysis above, we found that the rock pillar has the highest shock risk. Therefore, by studying the evolution law of the b value of 50 days before the "3.13" rockburst (the shock source is in the rock pillar), this section reveals the time precursory characteristics of the rockburst in the sandwiched rock pillar.

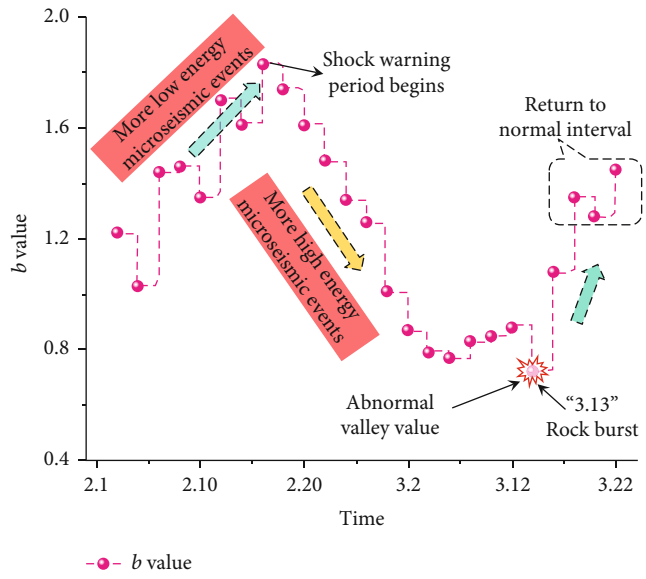

FIGURE 9: Variation of b values before and after the "3.13" rockburst.

The microseismic event data in the area with rock pillars from February 1 to March 22, 2015 were extracted to analyze the evolution law of the b value before and after the rock burst. The b value is calculated once every 2 d, and the change of the b value is shown in Figure 9. The b value gradually increased from February 1 to February 16. It shows that with the advance of the working face, the coal-rock mass is in the stage of small-scale fracture development, and the low-energy microseismic events account for a large proportion. From February 17 to March 4, the b value decreased, and the cracks in coal-rock mass gradually expanded and penetrated. A large number of high-energy microseismic events also released some energy. This phenomenon is a sign of coal-rock mass shock instability. The rockburst occurred on March 13, and then, the b value gradually increased and returned to the normal level. Therefore, we believe that when the b value of the rock pillar increases and then suddenly decreases, it means that the rock pillar enters the shock early warning period. Rockburst will occur within 25 days after entering the shock early warning period, and relevant measures shall be taken in time.

4.3. Time Characteristic Analysis of Microseismic Activity Parameters. In the mining process, the changing trend of cumulative apparent volume, energy index, Schmidt, and other indicators is an important parameter to characterize the stable state of coal-rock mass [25]. Relevant research shows that the sudden decrease of energy index and Schmidt and the increase of cumulative apparent volume are important precursory indicators of coal-rock mass instability [26]. The interval between the precursory indicators and rockburst in different mines is different. Therefore, by analyzing

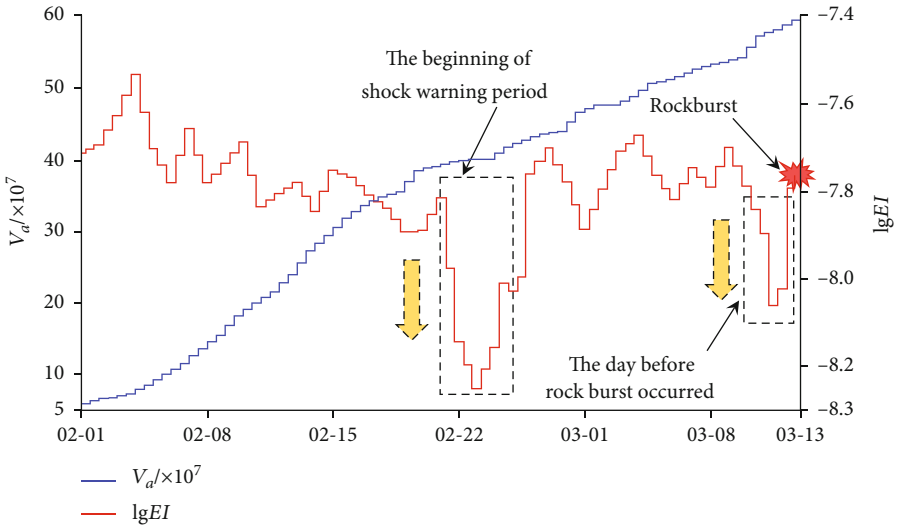

Figure 10: Variation of cumulative apparent volume and energy index.

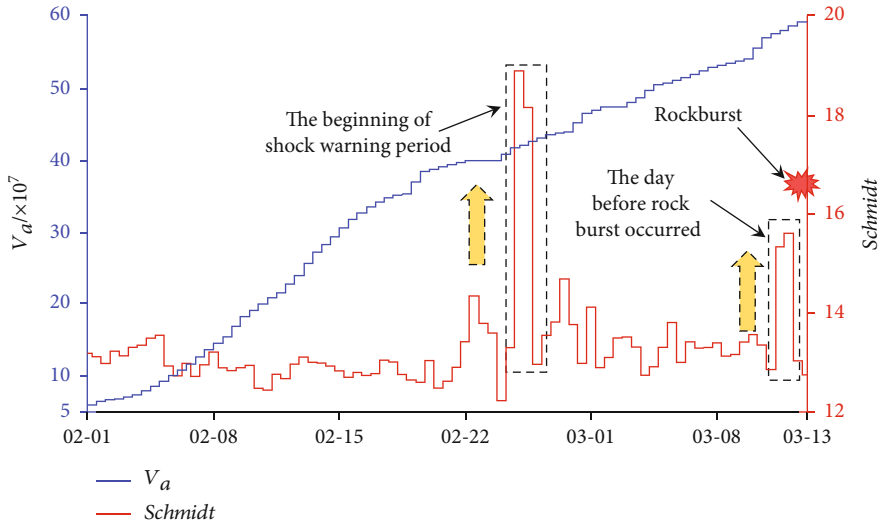

Figure 11: Variation of cumulative apparent volume and Schmidt.

the evolution law of cumulative apparent volume and energy index of the historical rockburst process, the precursory characteristics of rockburst in the south mining area can be effectively obtained. This is of great significance to effectively avoid rockbursts. The parameter characterization is shown in

$$V_a = \frac{M^2}{2\mu E}, \tag{2}$$

$$Sc_s = \frac{4\mu^2 \Delta V \Delta t(\bar{t}) \sum_{t_1}^{t_2} E}{\rho(\bar{X})^2 (M_{ij})^2}, \tag{3}$$

$$EI = \frac{E}{\bar{E}(M)}, \tag{4}$$

where M is the moment magnitude; μ is shear stiffness, N/m; ρ is the density of rock mass, kg/m^3; ΔV is the selected space, m^3; $\Delta t$is the time increment, s; E is microseismic energy, J; t is the average time difference of two consecutive microseismic events, s; X is the average distance of two consecutive microseismic events, m; and $E(M)$ is the average energy under the same seismic moment, J.

Taking "3.13" rockburst as an example, the change curve of cumulative apparent volume and energy index in the rock pillar before and after the rockburst is shown in Figure 10. The cumulative apparent volume increased slowly from February 1 to February 22, while the energy index fluctuated continuously. At this stage, the coal-rock mass is in a state of energy accumulation, and small-scale fractures are gradually developed. The energy index decreased rapidly on February 23, and the cumulative apparent volume was in the stage of continuous growth. Before the occurrence of the rockburst on March 13, the energy index decreased many times, and the cumulative apparent volume was always in the stage of continuous growth. Among them, the decline on February 22 is relatively the largest, which

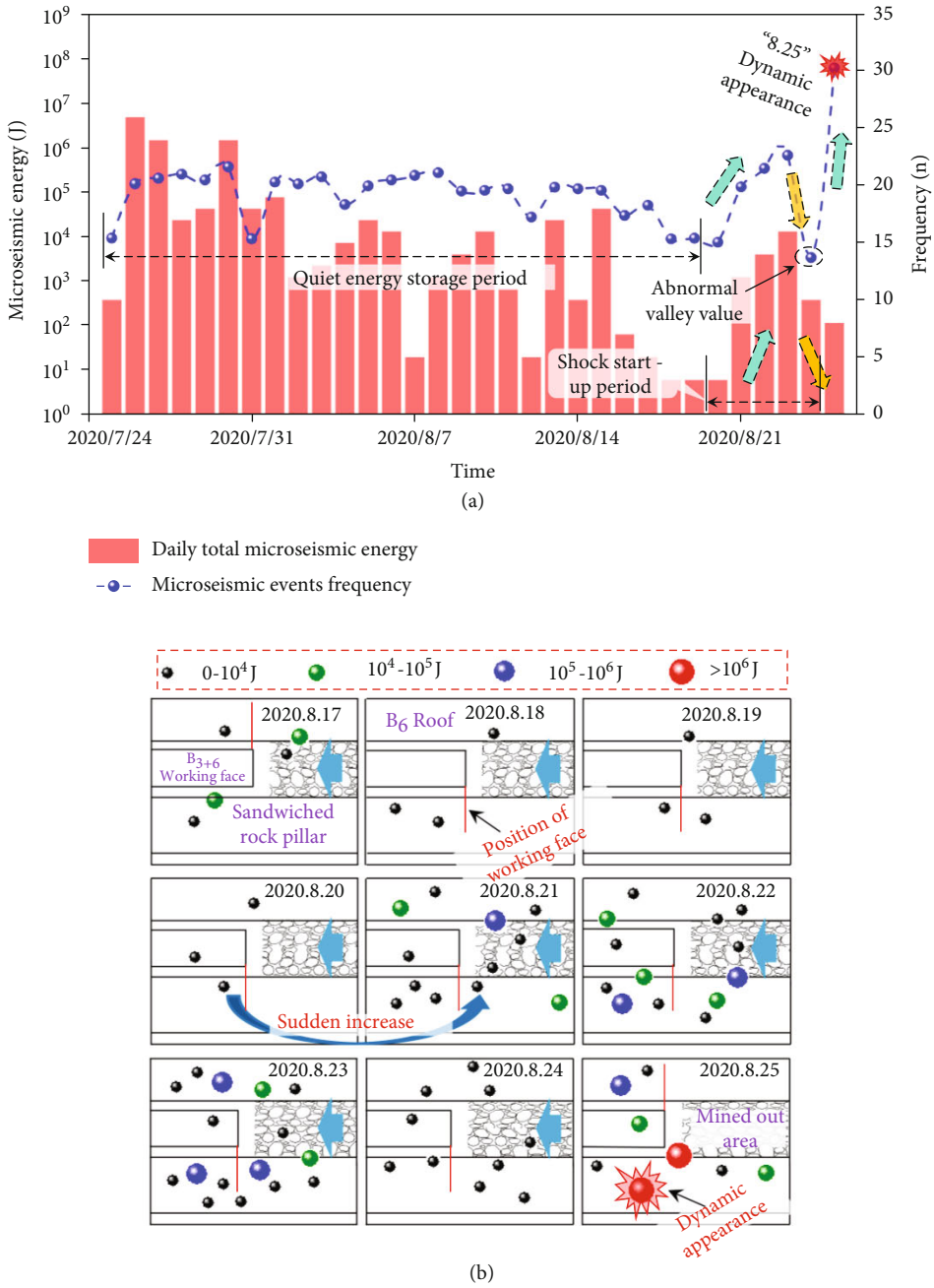

FIGURE 12: "Time-space-strength" evolution characteristics of microseismic events before "8.25" dynamic disaster. (a) Evolution characteristics of "energy-frequency" of microseismic events before "8.25" dynamic disaster. (b) Location of microseismic events before "8.25" dynamic disaster.

indicates that the rock mass has a trend of large-scale damage in this stage. It indicates that the shock warning period of the rock pillar has entered at this time. "3.13" rockburst occurred after 19 d. With the continuous advancement of the working face, the energy index decreased suddenly on March 11, and there was a large energy release on that day. This indicates that a large-scale rock mass fracture has occurred, which is also the beginning and warning of further potential damage. At this time, the coal-rock mass is in a state of stress softening, and the impact risk is great. The variation curve of cumulative apparent volume and Schmidt in the rock pillar is shown in Figure 11. The decrease of Schmidt is the largest on February 24, which can be determined as the beginning of the shock warning period in the rock pillar. The energy index began to rise normally on February 25, and the Schmidt fluctuated several times in a small range, indicating that the internal fractures of coal-rock mass gradually expanded at this stage. After February 25, the diffusion of microseismic events increased and the Schmidt decreased rapidly, indicating that the coal-rock mass had been unstable at this time. After 17 days, a high-energy shock source appeared in the rock pillar, and the rockburst occurred.

The above research shows that the evolution law of cumulative apparent volume, Schmidt, and energy index can be used to early warning the large-scale instability of rock mass. The significant decrease in energy index and the rapid increase of Schmidt can be judged as the beginning of the shock warning period. The shock risk of the Wudong Coal Mine is positively correlated with the decline rate of energy index, cumulative apparent volume, and the growth rate of the Schmidt number.

4.4. Determination of Shock Disaster-Causing Time of Rock Pillar. In the previous paper, the microseismic activity parameters such as the b value, energy index, cumulative apparent volume, and Schmidt before and after the "3.13" rockburst were deeply analyzed. Based on the evolution characteristics of different microseismic activity parameters, three different shock early warning periods are obtained. Among them, it takes a long time to determine whether the b value is in a continuous decline state. Misjudgment may occur only by using the short-term decline of the b value as a distinguishing index. According to the actual situation of mining, the 25 d (disaster-causing time after entering the shock early warning period) calculated based on the b value is earlier, which affects the normal production of the mine. Combined with the evolution characteristics of energy index, cumulative apparent volume, and Schmidt, it is considered that rockburst will occur within 19 days after entering the shock early warning period. After entering this period, the mine needs to strengthen the stress monitoring of the rock pillar. Attention should be paid to the change of rock mass and abnormal vibration and pressure relief control measures. When necessary, mining should be stopped and personnel evacuated as soon as possible.

5. Verification of Onsite Early Warning Results

On August 25, 2020, a dynamic disaster event occurred in the southern mining area. The seismic focus was located in the rock pillar. As shown in Figure 12, the dynamic disaster shows the "time-intensity" characteristics of microseismic activities before and after the occurrence. It can be seen from the figure that the total daily energy and frequency of microseisms suddenly increased and decreased simultaneously 5 days before the dynamic disaster, and the total daily energy was in an abnormal valley. At the same time, it can be seen from the location map that the number of microseismic events increased abnormally. The average number of microseismic events in the previous day was 4, while the average number of daily microseismic events accumulated abnormally was 12, with an increased rate of 66.7%. Therefore, we carried out effective early warning on the day when the dynamic disaster appeared, organized personnel evacuation, and avoided casualties. It is proved again that the coal-rock mass experiences the process of "stable development-unstable expansion-instantaneous shock failure" before the dynamic disaster [27]. The "time-intensity" early warning index based on microseismic activity proposed in this paper has a good early warning effect.

6. Conclusions

(1) Based on the field-measured microseismic data, this paper reveals the evolution law of "spatio-tempo-intension" before and after the three rockbursts. It is found that the rock pillar is the primary inducement of rockburst in space. The precursory indexes of rockburst are proposed from the aspects of time scale and intensity index: ① within 5 days before rockburst, the total daily energy, and frequency of microseisms suddenly rise and fall rapidly at the same time, and the total daily energy decreases to an abnormal valley. ② The abnormal growth rate of microseismic events exceeds 60% in a certain stage, and "induced shock events" appear

(2) By analyzing the "magnitude-frequency" relationship and the change of b value in a certain monitoring period, it is judged that the microseismic activity in the southern mining area of the Wudong Coal Mine is mainly of the stress migration type. Faults and other geological structures have little influence on them. With the continuous mining, the b value of the rock pillar decreased by 23.9%, the b value of the B6 roof decreased by 9.3%, and the b value of the B3+6 coal seam increased by 5.9%. The shock risk of the Wudong Coal Mine is positively correlated with the decline rate of energy index, cumulative apparent volume, and the growth rate of Schmidt

(3) It is determined that the rockburst will occur within 19 days after entering the early warning period in the southern mining area. At the same time, the prediction example of the "8.25" rockburst shows that the method has a good prediction effect on rockburst in a strong meizoseismal area. The research results can provide a reference for the prevention and control of rockburst in mines under the same conditions

Data Availability

The data that support the findings of this study are available from the corresponding author upon reasonable request.

Conflicts of Interest

No conflict of interest exists in the submission of this manuscript.

Authors' Contributions

Huicong Xu, Xingping Lai, Pengfei Shan, and Shuai Zhang contributed to the conception and design of the study. Zheng Wu, Rui Bai, and Haidong Xu contributed to the analysis and interpretation of data. Huicong Xu, Xingping Lai, Pengfei Shan, Qifeng Guo, and Shuai Zhang contributed to writing the manuscript. All authors provided final approval of the manuscript and agree to be accountable for all aspects of the work. The manuscript is approved by all authors for publication.

Acknowledgments

The study has been supported by the basic research program of the Natural Science in Shaanxi Province (No. S2019-JC-LH-QY-SM-0102), the National Natural Science Foundation of China (No. 51904227), the Key Laboratory of Western Mine Exploitation and Hazard Prevention, Ministry of Education (SKLCRKF1901), the Key Research and Development Program of Shaanxi Province (No. 2018ZDXM-SF-018), and the Key R&D Project of Yulin National High-tech Industrial Development Zone (2D-2021-01). Support from these agencies is gratefully acknowledged.

References

[1] X. Lai, F. Cui, J. Cao, and Y. L. Kang, "Analysis on characteristics of overlying rock caving and fissure conductive water in top-coal caving working face at three soft coal seam," *Journal of China Coal Society*, vol. 42, no. 1, pp. 148–154, 2017.

[2] H. Xu, X. Lai, P. Shan et al., "Energy dissimilation characteristics and shock mechanism of coal-rock mass induced in steeply-inclined mining: comparison based on physical simulation and numerical calculation," *Acta Geotechnica*, 2022.

[3] W. Guo, G. Gao, and X. Wang, "Characteristics of temporal-spatial distribution of annual seismic risk region in Xinjiang," *Inland Earthquake*, vol. 1, pp. 34–42, 2008.

[4] H. Liu, B. Zhang, X. Li et al., "Research on roof damage mechanism and control technology of gob-side entry retaining under close distance gob," *Engineering Failure Analysis*, vol. 138, no. 5, article 106331, 2022.

[5] X. Wang, C. Zhang, J. Deng, C. Su, and Z. Gao, "Analysis of factors influencing miners' unsafe behaviors in intelligent mines using a novel hybrid MCDM model," *International Journal of Environmental Research and Public Health*, vol. 19, no. 12, p. 7368, 2022.

[6] X. Li, S. Chen, S. Liu, and Z.-h. Li, "AE waveform characteristics of rock mass under uniaxial loading based on Hilbert-Huang transform," *Journal of Central South University*, vol. 28, no. 6, pp. 1843–1856, 2021.

[7] C. Zhang, X. Li, L. Dong, and X. B. Li, "Intelligent prediction of rock mass instability based on microseismic monitoring," *Journal of Safety Science and Technology*, vol. 12, no. 3, pp. 5–9, 2016.

[8] L. Dong, H. Qingchun, X. Tong, and Y. Liu, "Velocity-free MS/AE source location method for three-dimensional hole- containing structures," *Engineering*, vol. 6, no. 7, pp. 827–834, 2020.

[9] X. Li, S. Chen, Q. Zhang, X. Gao, and F. Feng, "Research on theory, simulation and measurement of stress behavior under regenerated roof condition," *Geomechanics and Engineering*, vol. 26, no. 1, pp. 49–61, 2021.

[10] E. Zhang, Q. Zhu, H. Miao, L. Gao, H. Chao, and Z. Zhang, "Study on monitoring and predicting of mine ground pressure activities based on microseismic technology," *Metal Mine*, vol. 8, pp. 172–181, 2020.

[11] R. Xue, Z. Liang, N. Xu, and L. Dong, "Rockburst prediction and stability analysis of the access tunnel in the main powerhouse of a hydropower station based on microseismic monitoring," *International Journal of Rock Mechanics and Mining Sciences*, vol. 126, article 104174, 2020.

[12] Y. Wang, C. A. Tang, L. Tang et al., "Microseismicity characteristics before and after a rockburst and mechanisms of intermittent rockbursts in a water diversion tunnel," *Rock Mechanics and Rock Engineering*, vol. 55, no. 1, pp. 341–361, 2021.

[13] G. Cheng, T. Ma, C. Tang, H. Liu, and S. Wang, "A zoning model for coal mining - induced strata movement based on microseismic monitoring," *International Journal of Mining Science and Technology*, vol. 94, pp. 123–138, 2017.

[14] X. Lai, H. Sun, P. Shan, M. F. Cai, F. H. Ren, and W. H. Tan, "Comprehensive evaluation of high-steep slope stability and optimal high-steep slope design by 3D physical modeling," *International Journal of Minerals, Metallurgy and Materials*, vol. 22, no. 1, pp. 1–11, 2015.

[15] X. Lai, C. Jia, F. Cui et al., "Microseismic energy distribution and impact risk analysis of complex heterogeneous spatial evolution of extra-thick layered strata," *Scientific Reports*, vol. 12, article 10832, 2022.

[16] W. Zhenhua, P. Pan, J. Chen, X. Liu, S. Miao, and P. Yu, "Mechanism of rock bursts induced by the synthetic action of "roof bending and rock pillar prying" in subvertical extra-thick coal *seams*," *Earth Science*, vol. 9, no. 3, 2021.

[17] X. Lai, X. Huicong, J. Chen et al., "Research on energy dissimilation characteristics and control method of sandwiched rock pillar by steeply inclined mining," *Journal of Mining & Safety Engineering*, vol. 38, no. 3, pp. 429–438, 2021.

[18] C. Lyu, J. Liu, Y. Ren, C. Liang, and Y. Zeng, "Mechanical characteristics and permeability evolution of salt rock under thermal-hydro-mechanical (THM) coupling condition," *Engineering Geology*, vol. 302, p. 106633, 2022.

[19] H. Xu, X. Lai, S. Zhang et al., "Multiscale intelligent inversion of water-conducting fractured zone in coal mine based on elastic modulus calibration rate response and its application - a case study of Ningdong mining area," *Lithosphere*, vol. 2021, article 7657143, 16 pages, 2021.

[20] C. P. Lu, G. J. Liu, Y. Liu, N. Zhang, J. H. Xue, and L. Zhang, "Microseismic multi-parameter characteristics of rockburst hazard induced by hard roof fall and high stress concentration," *International Journal of Rock Mechanics & Mining Sciences*, vol. 76, pp. 18–32, 2015.

[21] M. Cai, P. K. Kaiser, and C. D. Martin, "Quantification of rock mass damage in underground excavations from microseismic event monitoring," *International Journal of Rock Mechanics & Mining Sciences*, vol. 38, no. 8, pp. 1135–1145, 2001.

[22] X. Bao and D. W. Eaton, "Fault activation by hydraulic fracturing in western Canada," *Science*, vol. 354, no. 6318, pp. 1406–1409, 2016.

[23] S. J. Gibowicz and A. Kijko, *An Introduction to Mining Seismology*, Academic Press, New York, 1994.

[24] M. R. Hudyma, *Analysis and interpretation of clusters of seismic events in mines, [Ph. D. thesis]*, University of Western Australia, Perth, Australia, 2008.

[25] J. Liu, X. Feng, Y. Li, S.-d. Xu, and Y. Sheng, "Studies on temporal and spatial variation of microseismic activities in a deep

metal mine," *International Journal of Rock Mechanics & Mining Sciences*, vol. 60, pp. 171–179, 2013.

[26] C. Wang, "Identification of early-warning key point for rock-mass instability using acoustic emission/microseismic activity monitoring," *International Journal of Rock Mechanics & Mining Sciences*, vol. 71, pp. 171–175, 2014.

[27] L. Yang, *Study on microseismic monitoring and key strata breaking of high-intensity mining in Western China, [Ph. D. thesis]*, Northeastern University, Shenyang, China, 2017.